Seasonal Variability of Aircraft Trajectories reducing NO_x-climate Impacts under a Multitude of Weather Patterns

Federica Castino, Feijia Yin, Volker Grewe
Delft University of Technology
Faculty of Aerospace Engineering
Delft, The Netherlands
f.castino@tudelft.nl

Hiroshi Yamashita, Sigrun Matthes,
Sabine Baumann, Simone Dietmüller
Deutsches Zentrum für Luft- und Raumfahrt
Institut für Physik der Atmosphäre
Wessling, Germany

Manuel Soler, Abolfazl Simorgh
U. Carlos III de Madrid
Department of Bioeng. and Aerospace Engineering
Madrid, Spain

Florian Linke, Benjamin Lührs
Hamburg University of Technology
Institute of Air Transportation Systems
Hamburg, Germany

***Abstract*—Air traffic contributes to global warming through CO_2 and non-CO_2 effects, including the impact of NO_x emissions on atmospheric ozone and methane, formation of contrails, and changes in the amount of stratospheric water vapour. The climate impact of non-CO_2 effects is highly dependent on the background atmospheric conditions at the time and location of emission. Therefore, there is the potential of mitigating the climate impact of aviation by optimizing the aircraft trajectories. In the present paper, we focus on the properties of alternative trajectories which have the potential to minimize the climate impact of NO_x emissions, under a multitude of weather patterns. This study aims at enhancing the understanding of the relation between NO_x-climate impacts and routing strategies, by employing the European Center Hamburg general circulation model (ECHAM) and the Modular Earth Submodel System (MESSy) Atmospheric Chemistry (EMAC) model. To this end, we conduct 1-year simulations with the air traffic submodel AirTraf 2.0, coupled to the EMAC model. We optimize 85 European flights, considering the atmospheric conditions at the time and location of the flight, to calculate the expected climate impact from the emitted species through a set of prototype algorithmic Climate Change Functions (aCCFs). The mean flight altitudes of NO_x-climate optimal trajectories showed seasonal and latitudinal dependencies. We found that the potential of reducing ozone effects from aviation NO_x is subjected to a strong seasonal cycle, reaching a minimum in summer.**

***Keywords*—air traffic management; climate impact reduction; nitrogen oxides emissions; aircraft trajectories optimization.**

I. Introduction

Air traffic is estimated to have contributed to about 5% of the total anthropogenic global warming [1]–[3]. Its demand is expected to recover from the effects of the COVID-19 pandemic, achieving higher growth rates than other transport modes [4]–[6]. As a consequence, it is crucial to reduce the climate impact of aviation. Aircraft emissions perturb the background atmospheric conditions through various mechanisms: the main processes are (1) the formation, spreading and persistence of contrail cirrus, (2) the perturbation on ozone, methane, and stratospheric water vapour caused by NO_x emissions, (3) emission of green-house gases, such as CO_2 and H_2O, (4) aerosol interactions with radiation and clouds [2], [3]. Local atmospheric conditions play a crucial role in determining the magnitude, and even the sign, of the radiative forcing terms due to the non-CO_2 effects, which account for about 2/3 of the net aviation effective radiative forcing [5]. In particular, the impact of NO_x emissions on climate has been shown to be highly dependent on cruise altitude and geographical location of the aircraft [7], [8]. Therefore, previous studies highlighted the potential of mitigating the climate impact of aviation by optimizing the aircraft trajectories [9]–[12].

Earth System Models have been employed to evaluate the mitigation potential of aircraft trajectory optimization. For example, the REACT4C research project developed the concept of *climate change functions*, to represent the dependency of the climate impact of a specific emission on its time and location [13]. However, this approach requires large computational costs, limiting the number of weather patterns that can be analyzed. To address this issue, algorithmic Climate Change Functions (aCCFs, [14]) were developed during the ATM4E SESAR-ER project (http://www.atm4e.eu/). These functions take as input instantaneous weather data at the time and location of emission, and allow to obtain an approximation of the Average Temperature Response over a time horizon of 20 years (ATR20, [13]). To measure the climate impact, a climate metrics should be defined, which resembles the respective cli-

mate objective [15]. In general, they vary with type of emission (pulse, sustained, or future emission scenarios), metric (e.g, warming potential, or average temperature response), and time horizon (20, 50, or 100 years). Here, the ATR20 is defined as the mean temperature change over a time horizon of 20 years [13].

The FlyATM4E project (https://flyatm4e.eu/) is applying these concepts to evaluate the mitigation potential of climate-optimized routes. In particular, one of the objectives of FlyATM4E is the identification of trajectories leading to a significant reduction of aviation climate impact, while leaving the economic costs nearly unchanged. The potential of finding these conditions in aviation has been shown by previous studies [9], [16], [17]. However, these studies usually focused on a limited number of representative weather patterns, or on specific regions of the airspace. Within FlyATM4E, we aim at identifying and analyzing optimized trajectories in the European airspace, under a multitude of weather patterns.

In this paper, we present our preliminary results, that we obtained during the first steps towards this objective. Firstly, we investigated the maximum feasible reduction of the climate impact from the aircraft emitted species, as simulated by our model. In particular, here we focus (1) on the effects of optimizing aircraft trajectories w.r.t. the impact of their NO_x emissions on climate, and (2) on the seasonal variability of these optimised trajectories, caused by the natural atmospheric variability. We present the results obtained during 1-year simulations, employing a set of prototype aCCFs to evaluate the climate impact of aircraft emissions. The aCCFs of ozone and methane were used to optimize the trajectories w.r.t. the climate impact of NO_x emissions, and to compare the difference with the NO_x-climate impact of *"cost-optimal"* trajectories. We conducted simulations from 1 December 2015 to 1 December 2016 with the ECHAM/MESSy Atmospheric Chemistry (EMAC) model (Section II). The model output is analyzed in Section III, and our results are discussed in Section IV. To conclude, we present our plans to further explore the mitigation potential of optimizing aircraft trajectories w.r.t. the climate impact of their emitted species (Section V).

II. Methods

A. Base model

The EMAC model is a numerical chemistry and climate simulation system that includes sub-models describing tropospheric and middle atmosphere processes and their interaction with oceans, land and human influences [18]. It uses the second version of the Modular Earth Submodel System (MESSy2) to link multi-institutional computer codes. The core atmospheric model is the 5th generation European Centre Hamburg general circulation model (ECHAM5, [19]). For the present study we applied EMAC (ECHAM5 version 5.3.02, MESSy version 2.54.0) in the T42L31ECMWF-resolution, i.e. with a spherical truncation of T42 (corresponding to a quadratic Gaussian grid of approx. 2.8 by 2.8 degrees in latitude and longitude) with 31 vertical hybrid pressure levels (up to 10 hPa $\sim$ 30 km of altitude). We applied a time step of 20 minutes, and we set the simulation duration to 1 year (from 1 Dec. 2015 to 1 Dec. 2016). The simulations were nudged down to the surface towards the ECMWF ERA-Interim reanalysis data [20]. The applied model setup comprised the submodels ACCF [21], CONTRAIL [22], and AIRTRAF [23]. Note that these sub-models are currently under development (further information on their status can be found at https://www.messy-interface.org). Therefore, in this study, we illustrate the preliminary results obtained using the current versions of these sub-models, to analyze the model behaviour under different routing strategies. Table I summarizes the settings of the model that were employed to run our yearly simulations.

TABLE I. Summary of the model setup employed in our simulations.

	ECHAM5
Horizontal resolution	T42 (2.81° × 2.81°)
Vertical resolution	L31ECMWF (31 vertical pressure levels up to 10 hPa $\sim$ 30 km)
Time step	20 min
Duration	1 year (from 1 Dec. 2015 to 1 Dec. 2016)
	AirTraf
Flight-plan	85 flights in the European airspace (ATM4E flight plan on 2015-12-18 with all A33x aircraft models)
Waypoints	101
Optim. Objectives	SOC, $ATR20_{NO_x}$ ($ATR20_{tot}$, $f_{cost\text{-}clim.}$)

B. Sub-model AirTraf

In our simulations, air traffic is simulated by the EMAC sub-model AirTraf 2.0 [23]. This model optimizes aircraft routes based on the calculated weather information provided by EMAC. During the optimization steps, a genetic algorithm (ARMOGA, [24]) provides the coordinates of eight control points (three along the projection on the Earth, and five in the vertical cross section), which determine the B-spline curve representing the flight trajectory (Figure 1, from [25]). AirTraf only considers the cruise phase of the flight, and the vertical control points can vary between FL290 and FL410 ($\sim$ 8.8 - 12.5 km). The model uses 101 waypoints (Table I) to divide each B-spline into segments, at which the flight properties are calculated for analysis and output [25]. Various routing strategies are available: each option optimizes a specific objective function, e.g. representing fuel used, operating cost, or the climate impact of a flight. The sub-model successfully minimizes the selected optimization objective [23].

A daily flight-plan, subset of a larger European flight-plan, is repeated on every simulation day. This subset includes only A33x aircraft models, taking into account that the AirTraf sub-model is currently configured for this aircraft type [23]. The flight-plan includes 65 Origin-Destination (OD) pairs, and their relative departure times throughout the day. A fraction

of these OD pairs are repeated multiple times each day, at different departure times. As a result, AirTraf optimizes a total of 85 flights on each simulation day.

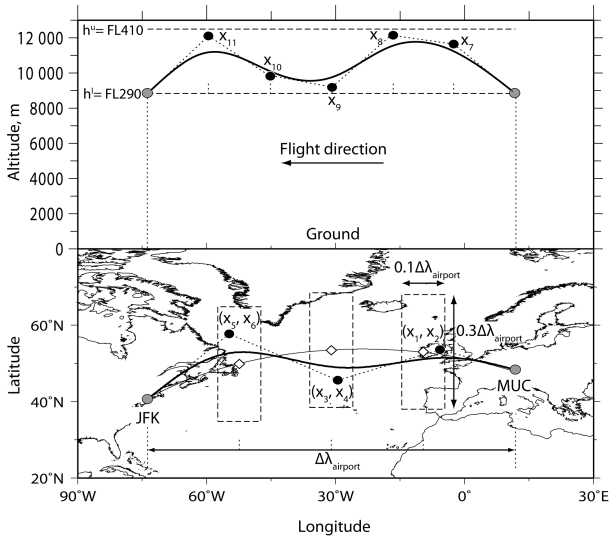

Figure 1. Geometry definition of the flight trajectory in the AirTraf sub-model, from Yamashita et al., 2016 [25]. A trajectory from MUC to JFK is used as example (bold solid lines). Top: the vertical cross section; the dashed lines indicate the lower/upper variable bounds in altitude. Bottom: projection on the Earth; the dashed boxes define the rectangular domains of the three control points.

C. Routing optimization strategies

We conducted simulations with the model setup described in the previous paragraphs, varying only the route optimization strategy. In particular, we consider the following options:

- *cost-optimal trajectories*, minimizing the Simple Operational Costs (SOC). Note that we use a simplified definition of the operational costs, as the aim of this optimization strategy is to take into account both flight time and fuel use. Therefore, the objective function values are calculated with the following formula [26], [27]:

$$\mathrm{SOC} = c_t \sum_{i=1}^{n_{\mathrm{wp}}-1} \mathrm{TIME}_i + c_f \sum_{i=1}^{n_{\mathrm{wp}}-1} \mathrm{FUEL}_i \qquad (1)$$

  where $n_{\mathrm{wp}} = 101$ are the number of waypoints; TIME_i and FUEL_i are flight time and fuel used at the i^{th} flight segment; c_t [$\$/s$] and c_f [$\$/kg$] are the unit time and unit fuel costs, respectively, assuming the values $c_t = 0.75$ $\$/s$ and $c_f = 0.51$ $\$/kg$ [23], [28].
- *NO_x-climate optimal trajectories*, minimizing the climate impact from NO_x emissions. This is represented by the sum of the ozone and methane effects, which are individually computed by the model using a set of prototype aCCFs [14], [21], [23]:

$$\mathrm{ATR20}_{\mathrm{NO_x}} = \mathrm{ATR20}_{\mathrm{O_3}} + \mathrm{ATR20}_{\mathrm{CH_4}} \qquad (2)$$

  Note that the aCCFs include the NO_x climate impact through the increase in ozone concentration and the reduction of methane concentration; they do not take into account the two feedback processes caused by the change in CH_4 concentration, affecting (1) primary mode ozone, and (2) the stratospheric water vapour [14].

III. Results

A. Changes in seasonal mean flight altitudes and horizontal paths

First of all, we look at how the aircraft trajectories change, when we minimize the climate impact of NO_x. Figure 2 compares cost-optimal and NO_x-climate optimal trajectories, averaged over the winter months (DJF). Analogue figures can be obtained for other seasons from our annual simulation, but they are not included here, as they show similar tendencies. The main difference between different seasons is the magnitude of the trajectory variations, as we discuss in the next paragraph (III-B).

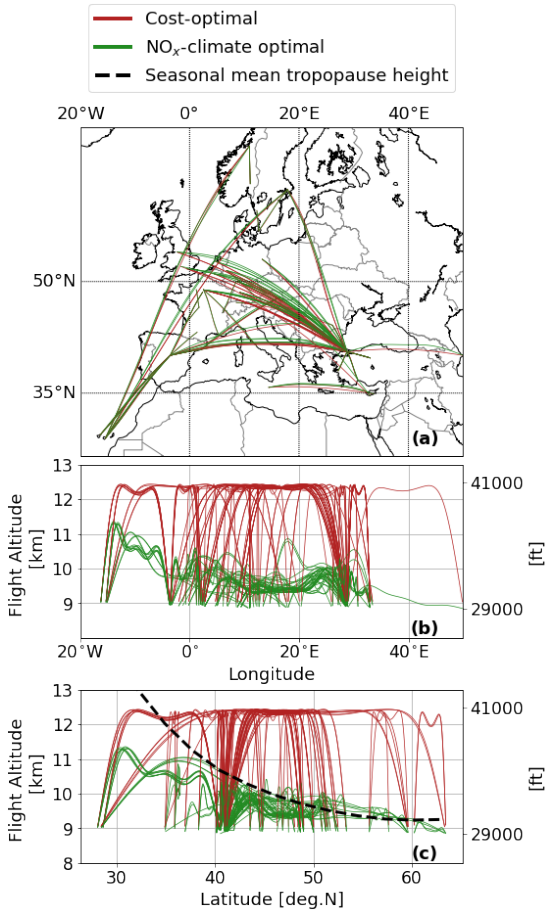

Figure 2. Comparison between vertical profiles and horizontal paths of flights optimized w.r.t. NO_x-climate impact (green lines) or Simple Operating Cost (red lines), averaged over the winter months (DJF). The top panel (a) shows the winter seasonal mean horizontal paths. The lower panels represent the winter seasonal mean flight altitude vs. longitude (b) and latitude (c). Each curve corresponds to a specific city-pair included in the flight-plan. Panel (c) includes the seasonal mean tropopause height as reference (black, dashed line).

Figure 2a shows the changes in the seasonally averaged horizontal paths. In general, the winter mean NO_x-climate

optimal horizontal routes show a northward shift of the aircraft locations. This is in agreement with previous studies [29], which found a decrease in the impact of NO_x emissions towards higher latitudes.

Figures 2b and 2c illustrate the winter seasonal mean flight altitude vs. longitude and latitude, respectively. We can see that the seasonal mean flight altitudes are highly affected by the choice of the routing strategy. The simulations show that NO_x-climate optimal trajectories tend to fly at lower altitudes than cost-optimal trajectories. This is in line with our expectations, since cost-optimal trajectories minimize the sum of fuel use and flight time and, to reduce aerodynamic drag, high altitudes are preferred. In contrast, the trajectories minimizing NO_x effects generally prefer lower flight altitudes. This is because the residence time of O_3 at lower altitudes is shorter, due to a more efficient wash out, which reduces the warming effects. This tendency of *flying lower* is in line with results from previous studies on the relation between NO_x-climate impact and flight altitudes [8], [30]–[32].

Furthermore, in Figure 2c, we can observe that NO_x-climate optimal trajectories present a strong dependency on latitude, which is not visible in the cost-optimal option. Using the NO_x-climate optimization strategy, the flight altitude increases towards lower latitudes, following the increasing average height of the tropopause (black, dashed curve). This model behaviour can be expected, considering that the upper-troposphere is characterised by a sharp increase in the NO_x climate impact, related to a high ozone production rate [29]. Therefore, the location of the tropopause is crucial in determining the cruise altitude of NO_x-climate optimal trajectories. On the other hand, from Figure 2b, we can see that there appears to be no clear dependency of the optimal flight altitude on the longitude, especially if we look at 0°-30°E. The fact that we observe higher flight altitudes in the western side of Figure 2b is due to the distribution of the origin-destination pairs on the map (Figure 2a), since western flights are all located at low latitudes.

B. Time-evolution of changes in fuel use and flight time

Figure 3 shows the evolution of flight altitude, flight time, fuel use, and Simple Operating Cost during the year of simulation. A 7-days running average is applied. Figure 3a compares the flight altitude of cost-optimal (red) and NO_x-climate optimal (green) trajectories. We can see that there is no evident seasonal variability in the flight altitude of cost-optimal trajectories, as its values remain constant at 11.5-12 km throughout the year. On the other hand, the reduction in the cruise altitude of NO_x-climate optimal trajectories is larger in winter than in summer. This could be linked to the elevation of the average height of the tropopause during the summer season, which determines the cruise altitude of NO_x-climate optimal trajectories, as described in Section III-A. Moreover, the extension of the shaded area shows that the variability within the set of flights is larger using the NO_x-climate optimization strategy. Figure 3b shows that the evolution of fuel increase follows the same seasonality, since it is driven by the increase in aerodynamic drag caused by flying at lower altitudes. Lastly, we can observe that the relative changes in flight time are also larger in winter/spring than during summer/autumn months, but they are always negligible compared to the changes in fuel use. Therefore, the increase in SOC is driven by the increment in fuel use.

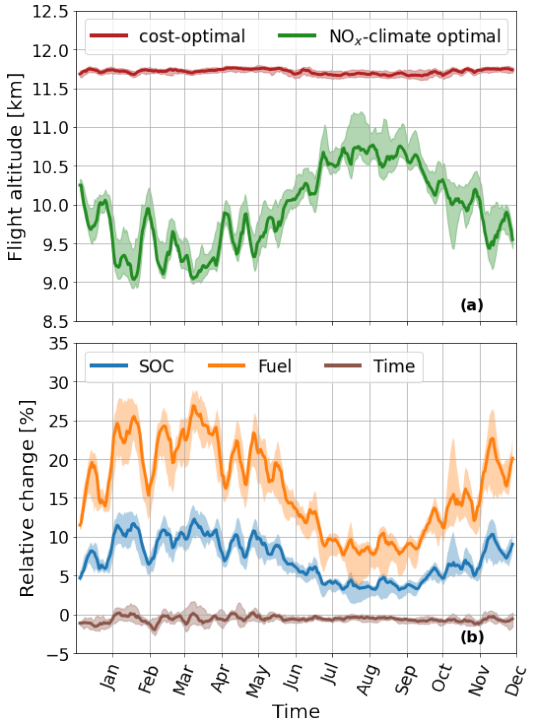

Figure 3. Evolution in time of: (a) flight altitude [km], averaged over the trajectory waypoints, comparing cost-optimal (red) and NO_x-climate optimal (green) trajectories; (b) relative change of Simple Operating Costs (blue), fuel (orange), and flight time (brown) of NO_x-climate optimal trajectories, w.r.t. cost-optimal ones. The thick lines indicate the median values over the 85 routes included in the flight plan. The shaded areas extend from the first to the third quartile. The curves represent the 7-days running average over the daily output values generated by the model.

C. Changes in NO_x climate impact

In this section, we look at the effects of minimizing $ATR20_{NO_x}$ on the two elements contributing to the NO_x-climate impact, i.e. the impact on $ATR20_{O_3}$ and $ATR20_{CH_4}$. Figure 4a shows the total aviation climate impact from NO_x emissions, combining ozone and methane effects. The magnitude is larger for ozone than for methane effects, thus the seasonality of the $ATR20_{O_3}$ relative variations (Figure 4b) emerges also in Figure 4a. We found that the impact of NO_x through ozone effects reaches a maximum in summer (Figure 4b), due to a higher photochemical activity, which is in agreement with previous studies [14], [32]. This seasonality is found for both optimization strategies.

During winter and spring, the $ATR20_{O_3}$ values are significantly reduced by NO_x-climate optimal trajectories. This could be due to the fact that vertical and latitudinal gradients in temperature and geopotential (input fields to calculate the ozone aCCF [14]) are larger in this period of the year. In

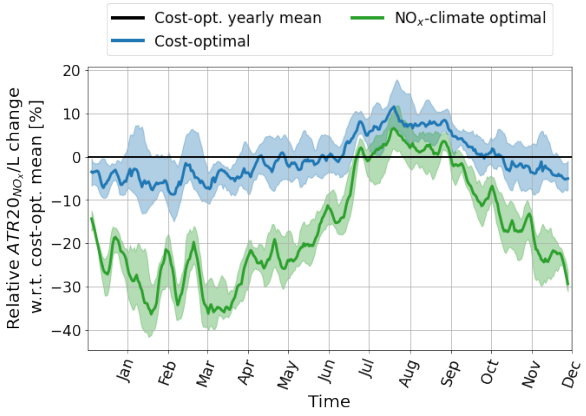

(a) Total aviation climate impact from NO_x emissions.

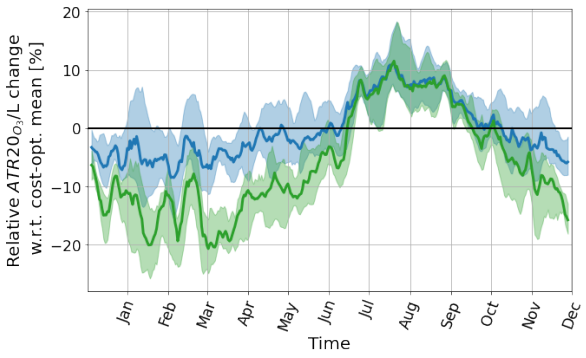

(b) NO_x-climate impact through ozone effects.

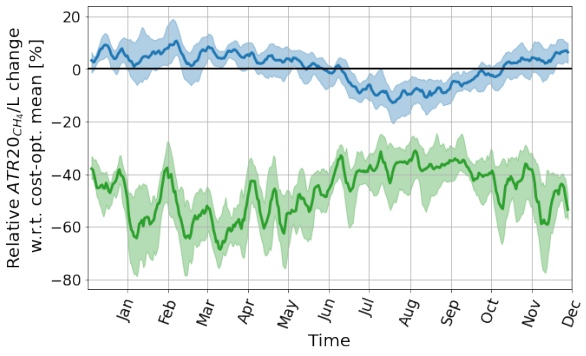

(c) NO_x-climate impact through methane effects.

Figure 4. Evolution in time of the relative change of aviation climate impact components, comparing cost-optimal (blue curves) and NO_x-climate optimal (green) trajectories. The yearly mean value from the cost-optimal strategy is chosen as reference (black line), and it assumes the values 1.9×10^{-13} K/km, 2.3×10^{-13} K/km, and -3.7×10^{-14} K/km, for panel (a), (b), and (c), respectively. The thick lines represent the median values over the 85 routes included in the flight plan, while the shaded regions extend from the first to the third quartile. The ATR20 values are weighted against the total flight length L. We perform a 7-days running average over the daily output values generated by the model.

winter/spring, the jet stream is stronger and located further south than during the summer [33], leading to sharper temperature and geopotential gradients over the European airspace. Therefore, the large mitigation potential in winter would be linked to (1) larger meridional mass exchange, hence large possibility to transport an air parcel to the tropics, and (2) larger difference in chemical activity between mid latitudes and tropics [34]. However, the $ATR20_{O_3}$ reduction is almost negligible in summer, when the jet stream is weaker and shifted northward.

Figure 4c shows that the cooling effects due to methane depletion are always enhanced by NO_x-climate optimal trajectories. It also emerges that NO_x-climate optimal and cost-optimal trajectories are characterized by opposite seasonal trends in $ATR20_{CH_4}$: the difference between the impact of the two strategies is largest in winter/spring, when $ATR20_{CH_4}$ reaches its maximum value in the cost-optimal scenario. Using the NO_x-climate optimization strategy, we can see that the maximum $ATR20_{CH_4}$ is reached during summer, when the enhancement of the cooling effects w.r.t. cost-optimal trajectories is reduced. Lastly, we notice that the daily variability of $ATR20_{CH_4}$ values across different city-pairs is larger for NO_x-climate optimal trajectories than it is for cost-optimal ones.

IV. Discussion

This study aims at enhancing the understanding of the relation between NO_x-climate impacts and routing strategies, exploring how the systematic application of a specific routing strategy in a global chemistry-climate model produces a comprehensive set of alternative trajectories which – under the strategy applied in this paper – are intended to have a smaller climate effect due to NO_x emissions. In this Section IV, we include two additional optimization strategies to (1) investigate the possible effects of NO_x-climate optimal trajectories on the other radiative forcing (RF) terms from aircraft emissions, and (2) introduce the next steps that are planned within our research project.

In this paper, we employed the aCCFs representing the effects of NO_x emissions on ozone and methane [14], [35]. At present, a full set of prototype aCCFs is available and implemented in the EMAC sub-model AirTraf, to represent the aviation climate impact of NO_x, contrails, water vapour, and CO_2. Therefore, the following optimization strategies are applicable in our simulations:

- *climate-optimal trajectories*, minimizing the total climate impact of a flight, measured as $ATR20_{tot}$. This objective function takes into account not only NO_x-climate impact, but also the climate impact of CO_2, H_2O, and day/night contrails effects, which are affected by higher uncertainty levels than $ATR20_{NO_x}$. Similarly to the evaluation of $ATR20_{NO_x}$, these terms are calculated separately, using the set of prototype aCCFs [14], [21], [23], and subsequently summed:

$$\begin{aligned} ATR20_{tot} = &ATR20_{NO_x} + ATR20_{cpc} + \\ &+ ATR20_{CO_2} + ATR20_{H_2O} \end{aligned} \tag{3}$$

  where $ATR20_{cpc}$, $ATR20_{CO_2}$, and $ATR20_{H_2O}$ represent the ATR20 from contrail potential coverage, carbon dioxide, and water vapour effects, respectively.
- *trade-off trajectories*, minimizing the weighted sum of SOC and $ATR20_{tot}$:

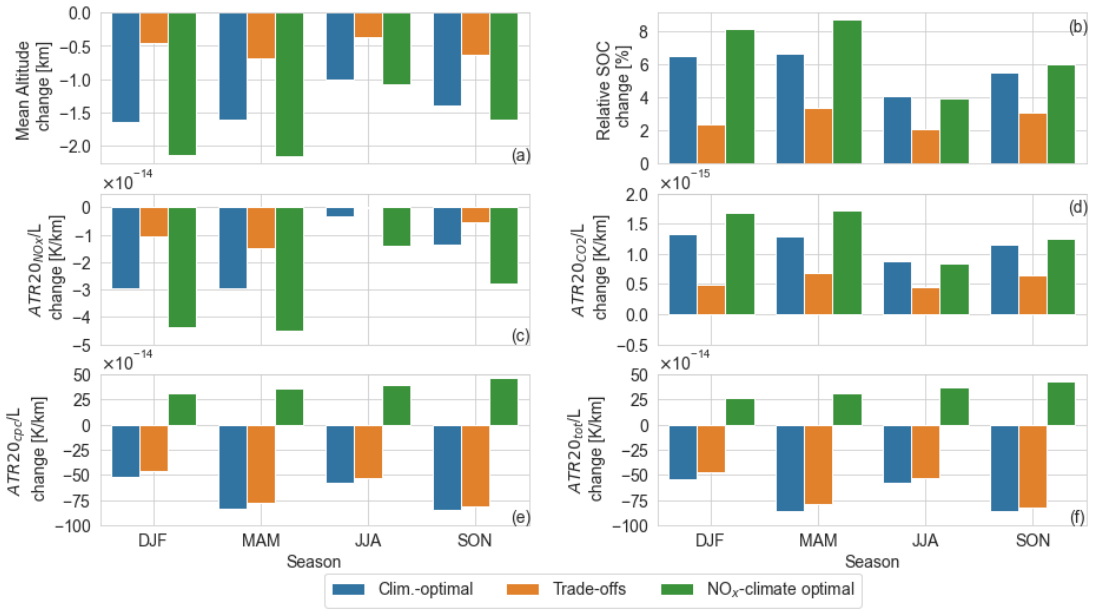

Figure 5. Seasonal mean values of the changes in flight altitude (a), SOC (b), the ATR20 from NO_x (c), CO_2 (d), contrail potential coverage (e), and the total ATR20 (f). We compare the variations w.r.t. cost-optimal trajectories of three different routing strategies: climate-optimal (blue bars), trade-offs (orange bars), and NO_x-climate optimal (green bars). Here we use the median values over the 85 city pairs included in the flight plan, before calculating the average over time.

$$f_{\text{cost-clim.}} = \alpha \text{ SOC} + \\ + (1-\alpha) k \text{ ATR20}_{\text{tot}} \tag{4}$$

where $\alpha \in [0,1]$ is a weight parameter, which determines the relative importance of SOC and $\text{ATR20}_{\text{tot}}$; k $[\$/K]$ is a conversion factor. In our simulations, we set $\alpha = 0.8$ to discourage increases in the SOC. To set the conversion factor k, the SOC and $\text{ATR20}_{\text{tot}}$ values of cost-optimal and climate-optimal trajectories are used to calculate the mean value of the following ratio [36]:

$$k = \frac{\text{SOC}_{\text{clim.-opt.}} - \text{SOC}_{\text{cost-opt.}}}{\text{ATR20}_{\text{cost-opt.}} - \text{ATR20}_{\text{clim.-opt.}}} \tag{5}$$

We set $k = 8.104302 \times 10^{12} \$/K$, which is a reference value obtained from free-running test simulations of the duration of 1 year, using the setup indicated in Table I.

These aCCFs are currently under verification, therefore it is not the aim of this paper to analyze the quantitative estimates calculated for *climate-optimal* and *trade-off* trajectories. On the other hand, they are included in this Discussion section to demonstrate the challenges that we are addressing in our research project, and the uncertainties affecting our results.

An assessment of changes in the overall performance of the alternative trajectories allows to compare trajectories from the three optimization strategies, and provides an overview on possible mitigation gains and trade-offs. Figure 5 summarizes the seasonal average variations in the main properties of the climate-, trade-off-, and NO_x-climate optimal trajectories, w.r.t. cost-optimal trajectories. Looking at panel 5f, we can see that NO_x-climate optimal trajectories do not reduce the total aviation climate impact in our simulations. In fact, contrail effects are the dominant contributor to the simulated changes in $\text{ATR20}_{\text{tot}}$ between different strategies (Figure 5e). On the other hand, if we include the $\text{ATR20}_{\text{tot}}$ values in the calculation of our Optimization Objective Function (i.e. in the climate-optimal and trade-off options), we achieve large reductions in $\text{ATR20}_{\text{tot}}$, especially in winter and spring months. These large variations are obtained by the model through the formation of cooling contrails, in agreement with [9]: in fact, the values of $\text{ATR20}_{\text{cpc}}$ using these strategies are often negative. It has to be noted here that direct compensation of a warming non-CO_2 effect by another (additional) non-CO_2 effects is facing the challenge that, at present, further knowledge on methods to quantify the response of the atmosphere-climate system is required, to ensure that two forcings really cancel out. What is significant to observe is that these large reductions in climate impact are achieved at lower increases in fuel use and flight time than those caused by NO_x-climate optimal trajectories, as shown by the variation in SOC in Figure 5b. In fact, Figure 5a shows that the mean flight altitude change is larger for NO_x-climate optimal trajectories, than for climate-optimal and trade-off solutions. On the other hand, these latter strategies are still reducing the NO_x-climate impact, especially in non-summer months (Figure 5c), even if the leading term of the optimization is $\text{ATR20}_{\text{cpc}}$. Lastly, we observe that all strategies lead to an increase in the impact of CO_2 emissions (Figure 5d), hence also fuel consumption, but this additional climate effect is compensated by the reduced RF of contrails and NO_x emissions.

Our calculation of SOC (Equation 1) comprises both costs of fuel and time, assuming a linear dependence between

costs of time and time of flight. If one would intend to consider extra costs due to delay time, a linear relationship would not be realistic. However, in our concept of alternative trajectories planning, these costs of time represent those costs due to longer working hours and usage of the airplane. Other costs, e.g. route charges are not included in the calculation of economic costs (SOC) in our analysis, as a simple relationship between time and costs would not be realistic. A detailed assessment of the regional strongly varying route charges and their influence on operating costs is beyond the scope of this study.

Please note that we rely on the aCCFs to calculate and compare the climate impact of different routing strategies. This innovative methodology has the advantage of significantly reducing the computational time, allowing to perform trajectory optimization. On-going research is addressing the source of uncertainties that affect the current climate impact estimates [37]. These are originated, for example, by (1) the calculation of the RF from the emitted species/contrails, and (2) the conversion from the RF values to the selected climate metric (ATR20). Moreover, the representation of atmospheric processes in the EMAC model is subjected to uncertainties, affecting the meteorological fields that are used as input for the aCCFs. Therefore, these sources of uncertainties must be taken into account interpreting the output of our model simulations.

The climate impact due to contrail effects is particularly sensitive to the background conditions simulated by the EMAC model: the meteorological fields affect the temporal and spatial distribution of contrails, as well as their radiative properties. This fact represents one of the challenges of optimizing the aircraft trajectories w.r.t. the total aviation climate impact.

On the other hand, our simulations appear to confirm the mitigation potential of aircraft trajectories optimization, which was already highlighted in previous studies [9], [11]. In particular, the final objective of our research is to identify trajectories leading to a significant reduction of the total aviation climate impact, while leaving fuel use and flight time nearly unchanged. To this end, we are currently improving the efficiency of the EMAC sub-model AirTraf for the resolution of Multi-Objective Optimization Problems, to identify trade-off trajectories using a more flexible approach, which will take into account the specific mitigation potential of different city pairs and weather patterns.

V. Conclusion

We used the EMAC sub-model AirTraf 2.0 to optimize aircraft routes within the European airspace, simulating the atmospheric conditions from 1 December 2015 to 1 December 2016. Subsequently, we analyzed the variability of the properties of aircraft trajectories characterizing cost-optimal and NO_x-climate optimal trajectories. Stressing again that we consider our current results as an initial study relying on prototype estimates of non-CO_2 effects, the main results and the next steps of our research are:

- The seasonal mean flight altitudes of NO_x-climate optimal trajectories are lower than those of cost-optimal ones. The difference between the two strategies follows a seasonal cycle, with a reduction in the variation during summer months, when the average tropopause height increases, and the potential of reducing NO_x effects decreases.
- The potential of reducing ozone effects from aviation NO_x is subjected to a strong seasonal cycle, reaching a minimum in summer.
- Taking into account other main effects of aviation emissions on climate (CO_2, H_2O, and contrails, as well as NO_x) the total climate impact might not be reduced by NO_x-climate optimal trajectories. However, this objective could be achieved by trajectories leading to a smaller increase in fuel use and flight time than NO_x-climate optimal trajectories, as we showed for the trade-off solutions mentioned in Section IV. This confirms the opportunity of developing our models to identify solutions leading to significant reductions in climate impact, without causing changes in cost that are not compensated by a decrease in the RF of aviation emissions.
- To address the previous remark, the optimization module of AirTraf is now under further development to improve its efficiency in solving Multi-Objective Optimization Problems. The new modules for Optimization and Decision-Making problems will be available in the next release of MESSy [38].
- And last, but not least, on-going research is addressing the sources of uncertainty that affect the current climate impact estimates, e.g. due to the aCCFs implementation, and to the meteorological fields at emission location. As this is one central research question in the FlyATM4E project, a systematic analysis is being conducted, analyzing such uncertainties as those originated by the calculation of the RF from the different components of aviation emissions, and the model representation of background atmospheric conditions [37].

Acknowledgment

The current study has been supported by the FlyATM4E project. This project has received funding from the SESAR Joint Undertaking under grant agreement No 891317 under European Union's Horizon 2020 research and innovation program.

References

[1] R. B. Skeie, J. Fuglestvedt, T. Berntsen, M. T. Lund, G. Myhre, and K. Rypdal, "Global temperature change from the transport sectors: Historical development and future scenarios," *Atmospheric Environment*, vol. 43, no. 39, pp. 6260–6270, 12 2009.

[2] D. S. Lee, G. Pitari, V. Grewe, K. Gierens, J. E. Penner, A. Petzold, M. J. Prather, U. Schumann, A. Bais, T. Berntsen, D. Iachetti, L. L. Lim, and R. Sausen, "Transport impacts on atmosphere and climate: Aviation," *Atmospheric Env.*, vol. 44, no. 37, pp. 4678–4734, 2010.

[3] G. P. Brasseur, M. Gupta, B. E. Anderson, S. Balasubramanian, S. Barrett, D. Duda, G. Fleming, P. M. Forster, J. Fuglestvedt, A. Gettelman, R. N. Halthore, S. D. Jacob, M. Z. Jacobson, A. Khodayari, K. N. Liou, M. T. Lund, R. C. Miake-Lye, P. Minnis, S. Olsen, J. E. Penner, R. Prinn, U. Schumann, H. B. Selkirk, A. Sokolov, N. Unger, P. Wolfe, H. W. Wong, D. W. Wuebbles, B. Yi, P. Yang, and C. Zhou, "Impact of aviation on climate: FAA's Aviation Climate Change Research Initiative

(ACCRI) phase II," *Bulletin of the American Meteorological Society*, vol. 97, no. 4, pp. 561–583, 2016.

[4] IPCC, V. Masson-Delmotte, P. Zhai, H.-O. Pörtner, D. Roberts, J. Skea, P. Shukla, A. Pirani, W. Moufouma-Okia, R. P. C. Péan, S. Connors, J. Matthews, Y. Chen, X. Zhou, M. Gomis, E. Lonnoy, T. Maycock, M. Tignor, and T. Waterfield, "Global Warming of 1.5°C. An IPCC Special Report on the impacts of global warming of 1.5°C above pre-industrial levels and related global greenhouse gas emission pathways, in the context of strengthening the global response to the threat of climate change," *In Press.*, 2018.

[5] D. S. Lee, D. W. Fahey, A. Skowron, M. R. Allen, U. Burkhardt, Q. Chen, S. J. Doherty, S. Freeman, P. M. Forster, J. Fuglestvedt, A. Gettelman, R. R. De León, L. L. Lim, M. T. Lund, R. J. Millar, B. Owen, J. E. Penner, G. Pitari, M. J. Prather, R. Sausen, and L. J. Wilcox, "The contribution of global aviation to anthropogenic climate forcing for 2000 to 2018," *Atmospheric Environment*, vol. 244, 2021.

[6] V. Grewe, A. Gangoli Rao, T. Grönstedt, C. Xisto, F. Linke, J. Melkert, J. Middel, B. Ohlenforst, S. Blakey, S. Christie, S. Matthes, and K. Dahlmann, "Evaluating the climate impact of aviation emission scenarios towards the Paris agreement including COVID-19 effects," *Nature Communications*, vol. 12, no. 1, 2021.

[7] M. O. Köhler, G. Rädel, K. P. Shine, H. L. Rogers, and J. A. Pyle, "Latitudinal variation of the effect of aviation NO_x emissions on atmospheric ozone and methane and related climate metrics," *Atmospheric Environment*, vol. 64, pp. 1–9, 2013.

[8] S. Matthes, L. Lim, U. Burkhardt, K. Dahlmann, S. Dietmüller, V. Grewe, A. S. Haslerud, J. Hendricks, B. Owen, G. Pitari, M. Righi, and A. Skowron, "Mitigation of Non-CO_2 Aviation's Climate Impact by Changing Cruise Altitudes," *Aerospace*, vol. 8, no. 2, pp. 1–20, 2021.

[9] V. Grewe, T. Champougny, S. Matthes, C. Frömming, S. Brinkop, O. A. Søvde, E. A. Irvine, and L. Halscheidt, "Reduction of the air traffic's contribution to climate change: A REACT4C case study," *Atmospheric Environment*, vol. 94, pp. 616–625, 2014.

[10] V. Grewe, S. Matthes, C. Frömming, S. Brinkop, P. Jöckel, K. Gierens, T. Champougny, J. Fuglestvedt, A. Haslerud, E. Irvine, and K. Shine, "Feasibility of climate-optimized air traffic routing for trans-Atlantic flights," *Environmental Research Letters*, vol. 12, no. 3, 2 2017.

[11] B. Lührs, F. Linke, S. Matthes, V. Grewe, and F. Yin, "Climate impact mitigation potential of European air traffic in a weather situation with strong contrail formation," *Aerospace*, vol. 8, no. 2, pp. 1–15, 2 2021.

[12] S. Matthes, B. Lührs, K. Dahlmann, V. Grewe, F. Linke, F. Yin, E. Klingaman, and K. P. Shine, "Climate-optimized trajectories and robust mitigation potential: Flying ATM4E," *Aerospace*, vol. 7, no. 11, pp. 1–15, 2020.

[13] V. Grewe, C. Frömming, S. Matthes, S. Brinkop, M. Ponater, S. Dietmüller, P. Jöckel, H. Garny, E. Tsati, K. Dahlmann, O. A. Søvde, J. Fuglestvedt, T. K. Berntsen, K. P. Shine, E. A. Irvine, T. Champougny, and P. Hullah, "Aircraft routing with minimal climate impact: The REACT4C climate cost function modelling approach (V1.0)," *Geoscientific Model Development*, vol. 7, no. 1, pp. 175–201, 1 2014.

[14] J. van Manen and V. Grewe, "Algorithmic climate change functions for the use in eco-efficient flight planning," *Transportation Research Part D: Transport and Environment*, vol. 67, pp. 388–405, 2019.

[15] V. Grewe and K. Dahlmann, "How ambiguous are climate metrics? And are we prepared to assess and compare the climate impact of new air traffic technologies?" *Atm. Environment*, vol. 106, pp. 373–374, 2015.

[16] U. Burkhardt, L. Bock, and A. Bier, "Mitigating the contrail cirrus climate impact by reducing aircraft soot number emissions," *npj Climate and Atmospheric Science*, vol. 1, no. 1, 2018.

[17] R. Teoh, U. Schumann, A. Majumdar, and M. E. Stettler, "Mitigating the Climate Forcing of Aircraft Contrails by Small-Scale Diversions and Technology Adoption," *Environmental Science and Technology*, vol. 54, no. 5, pp. 2941–2950, 2020.

[18] P. Jöckel, A. Kerkweg, A. Pozzer, R. Sander, H. Tost, H. Riede, A. Baumgaertner, S. Gromov, and B. Kern, "Development cycle 2 of the Modular Earth Submodel System (MESSy2)," *Geoscientific Model Development*, vol. 3, no. 2, pp. 717–752, 2010.

[19] E. Roeckner, G. Bäuml, L. Bonaventura, R. Brokopf, M. Esch, M. Giorgetta, S. Hagemann, I. Kirchner, L. Kornblueh, E. Manzini, A. Rhodin, U. Schlese, U. Schulzweida, and A. Tompkins, "The atmospheric general circulation model ECHAM 5. PART I: Model description." *Report / Max-Planck-Institut für Meteorologie*, no. 349, p. 349, 2003.

[20] D. P. Dee, S. M. Uppala, A. J. Simmons, P. Berrisford, P. Poli, S. Kobayashi, U. Andrae, M. A. Balmaseda, G. Balsamo, P. Bauer, P. Bechtold, A. C. M. Beljaars, L. van de Berg, J. Bidlot, N. Bormann, C. Delsol, R. Dragani, M. Fuentes, A. J. Geer, L. Haimberger, S. B. Healy, H. Hersbach, E. V. Hólm, L. Isaksen, P. Kållberg, M. Köhler, M. Matricardi, A. P. McNally, B. M. Monge-Sanz, J.-J. Morcrette, B.-K. Park, C. Peubey, P. de Rosnay, C. Tavolato, J.-N. Thépaut, and F. Vitart, "The ERA-Interim reanalysis: configuration and performance of the data assimilation system," *Quarterly Journal of the Royal Meteorological Society*, vol. 137, no. 656, pp. 553–597, apr 2011.

[21] F. Yin, V. Grewe, F. Castino, P. Rao, S. Matthes, H. Yamashita, K. Dahlmann, C. Frömming, S. Dietmüller, P. Peter, E. Klingaman, K. Shine, B. Lührs, and F. Linke, "Predicting the climate impact of aviation for en-route emissions: The algorithmic climate change function sub model ACCF 1.0 of EMAC 2.53," *in preparation, GMD*, 2021.

[22] C. Frömming, V. Grewe, S. Brinkop, and P. Jöckel, "Documentation of the EMAC submodels AIRTRAC 1.0 and CONTRAIL 1.0, supplementary material of Grewe et al., 2014b, 7, 175–201," *GMD*, 2014.

[23] H. Yamashita, F. Yin, V. Grewe, P. Jöckel, S. Matthes, B. Kern, K. Dahlmann, and C. Frömming, "Newly developed aircraft routing options for air traffic simulation in the chemistry–climate model EMAC 2.53: AirTraf 2.0," *GMD*, vol. 13, no. 10, pp. 4869–4890, 10 2020.

[24] D. Sasaki and S. Obayashi, "Efficient search for trade-offs by adaptive range multi-objective genetic algorithms," *Journal of Aerospace Computing, Information and Communication*, vol. 2, pp. 44–64, Jan. 2005.

[25] H. Yamashita, V. Grewe, P. Jöckel, F. Linke, M. Schaefer, and D. Sasaki, "Air traffic simulation in chemistry-climate model EMAC 2.41: AirTraf 1.0," *Geoscientific Model Devel.*, vol. 9, no. 9, pp. 3363–3392, 9 2016.

[26] A. Cook, G. Tanner, V. Williams, and G. Meise, "Dynamic cost indexing – Managing airline delay costs," *Journal of Air Transport Management*, vol. 15, no. 1, pp. 26–35, 1 2009.

[27] L. Marla, B. Vaaben, and C. Barnhart, "Integrated Disruption Management and Flight Planning to Trade Off Delays and Fuel Burn," *Transportation Science*, vol. 51, no. 1, pp. 88–111, 2 2017.

[28] M. A. Burris, "Cost index estimation," in *IATA 3rd Airline Cost Conference, Geneva, Switzerland*, 2015, p. 1–23.

[29] M. O. Köhler, G. Rädel, O. Dessens, K. P. Shine, H. L. Rogers, O. Wild, and J. A. Pyle, "Impact of perturbations to nitrogen oxide emissions from global aviation," *Journal of Geophysical Research Atmospheres*, vol. 113, no. 11, pp. 1–15, 2008.

[30] V. Grewe, M. Dameris, C. Fichter, and D. S. Lee, "Impact of aircraft NO_x emissions. Part 2: Effects of lowering the flight altitude," *Meteorologische Zeitschrift*, vol. 11, no. 3, pp. 197–205, aug 2002.

[31] C. Frömming, M. Ponater, K. Dahlmann, V. Grewe, D. S. Lee, and R. Sausen, "Aviation-induced radiative forcing and surface temperature change in dependency of the emission altitude," *Journal of Geophysical Research Atmospheres*, vol. 117, no. 19, pp. 1–15, 2012.

[32] O. A. Søvde, S. Matthes, A. Skowron, D. Iachetti, L. Lim, B. Owen, Ø. Hodnebrog, G. Di Genova, G. Pitari, D. S. Lee, G. Myhre, and I. S. Isaksen, "Aircraft emission mitigation by changing route altitude: A multi-model estimate of aircraft NO_x emission impact on O_3 photochemistry," *Atmospheric Environment*, vol. 95, pp. 468–479, 2014.

[33] C. L. Archer and K. Caldeira, "Historical trends in the jet streams," *Geophysical Research Letters*, vol. 35, no. 8, 2008.

[34] S. Rosanka, C. Frömming, and V. Grewe, "The impact of weather pattern and related transport processes on aviation's contribution to ozone and methane concentrations from NO_x emissions," *Atmospheric Chemistry and Physics*, no. x, pp. 1–20, 2020.

[35] F. Yin., V. Grewe., J. v. Manen, S. Matthes., H. Yamashita., F. Linke., and B. Lührs, "Verification of the ozone algorithmic climate change functions for predicting the short-term NO_x effects from aviation en-route," *Icrat*, pp. 1–8, June 2018.

[36] S. Matthes, V. Grewe, K. Dahlmann, C. Frömming, E. Irvine, L. Lim, F. Linke, B. Lührs, B. Owen, K. Shine, S. Stromatas, H. Yamashita, and F. Yin, "A concept for multi-criteria environmental assessment of aircraft trajectories," *Aerospace*, vol. 4, no. 3, 2017.

[37] M. Matthes, S. Dietmüller, S. Baumann, F. Castino, K. Dahlmann, D. González-Arribas, V. Grewe, F. Linke, B. Lührs, M. Meuser, A. Simorgh, M. Soler, H. Yamashita, and F. Yin, "Concept for identifying robust eco-efficient aircraft trajectories," *in preparation, Aerospace*, 2021.

[38] H. Yamashita, F. Castino, F. Yin, S. Matthes, V. Grewe, S. Dietmüller, P. Jöckel, and P. Rao, "Multi-objective flight trajectory optimization in EMAC: AirTraf 3.0," *in preparation, Geoscientific Model Development*, 2022.